Bergische Universität Wuppertal

Fachbereich Mathematik und Naturwissenschaften

Lehrstuhl für Angewandte Mathematik
und Numerische Mathematik

Preprint BUW-AMNA 03/01

Roland Pulch

Multi Time Scale Differential Equations for Simulating Frequency Modulated Signals

November 2003

http://www.math.uni-wuppertal.de/org/Num/

Multi Time Scale Differential Equations for Simulating Frequency Modulated Signals

R. Pulch

Bergische Universität Wuppertal, Fachbereich C,
Arbeitsgruppe Angewandte Mathematik / Numerische Mathematik,
Gaußstr. 20, D-42119 Wuppertal, Germany.

Abstract
Radio-frequency (RF) circuits produce quasiperiodic signals with widely separated time scales. In the case of autonomous time scales, frequency modulation occurs in addition to amplitude modulation. A multidimensional signal model yields an efficient numerical simulation by computations via a multirate partial differential algebraic equation (MPDAE) with periodic boundary conditions. We present a time domain method for these systems, which integrates along characteristic curves and thus is consistent with the inherent information transport. Moreover, we propose a special choice for additional boundary conditions, which are necessary to determine local frequencies. Test results confirm that the constructed techniques compute efficiently frequency modulated quasiperiodic signals in RF applications.

1 Introduction

The numerical simulation of electrical circuits is based on a network approach, which typically yields systems of *differential algebraic equations* (*DAEs*), see [2]. These systems describe the transient behaviour of all node voltages and some branch currents. In RF applications, circuits often include signals with largely differing time scales. Thus integrating the circuit's equations in time domain demands an enormous computational work, since the fastest rate limits the integration step size, whereas the slowest rate mostly decides the total time interval of the simulation.

A multidimensional signal model permits an alternative strategy by decoupling the separate time scales. Consequently, the DAE model of the circuit is transformed into a PDAE model, the *multirate partial differential algebraic equation* (*MPDAE*). Corresponding multiperiodic solutions yield the desired DAE solutions. Brachtendorf et al. [1] successfully applied this PDAE approach in frequency domain by a generalisation of harmonic balance. An analysis of the PDAE system exhibits an information transport along characteristic curves [8]. This structure enables a method of characteristics to compute multiperiodic solutions. The technique is efficient and robust for simulating MPDAE models, where the time scales are driven by input signals, see [9], and thus purely amplitude modulated responses with constant frequencies arise.

If autonomous time scales occur in addition to driven rates, then the signals may be frequency modulated, too. Narayan and Roychowdhury [7] generalised the multidimensional model to this case and introduced a *warped MPDAE* system. In contrast to the purely driven situation, an unknown local frequency function arises in addition to the multiperiodic solution. Consequently, an extra condition is required to determine uniquely the involved functions. Thus the multidimensional model is more complicated in the case of autonomous time scales.

In this paper, we tailor the method of characteristics to the warped MPDAE model. Thereby, just two time scales are considered, i.e. a forced and an autonomous rate, since modifications to several time scales are straightforward. In addition, we suggest a specific phase condition to fix the local frequency function. This condition produces additional boundary conditions in the method of characteristics. Furthermore, we develop a homotopy method, which shall secure the convergence of corresponding Newton iterations. The constructed method of characteristics is used to solve two classical test examples in circuit simulation, which represent systems of ordinary differential equations (ODEs). These ODE systems already indicate the appearance of autonomous time scales.

The paper is organised as follows. We outline the multidimensional model in Sect. 2. Then the corresponding warped MPDAE model is introduced. Analysing the information transport in the system, we construct a method of characteristics for the numerical solution in Sect. 4. Finally, test results using a Van der Pol and a Colpitt oscillator are illustrated in Sect. 5 and Sect. 6, respectively.

2 Multidimensional Signal Model

The purpose of the multidimensional model is to represent efficiently signals including widely separated time scales. As a simple instance, we consider the

amplitude modulated signal

$$v(t) = \left[1 + \tfrac{1}{2}\sin\left(\tfrac{2\pi}{T_1}t\right)\right]\sin\left(\tfrac{2\pi}{T_2}t\right) \tag{1}$$

with $T_1 \gg T_2$. Consequently, many time steps are required to resolve all oscillations of the fast rate T_2 during one slower rate T_1. However, we are able to change from the time-dependent signal (1) to a multidimensional representation, where each time scale is described by its own variable. Accordingly, we obtain the function

$$\hat{v}(t_1, t_2) = \left[1 + \tfrac{1}{2}\sin\left(\tfrac{2\pi}{T_1}t_1\right)\right]\sin\left(\tfrac{2\pi}{T_2}t_2\right), \tag{2}$$

which is biperiodic and thus given by its values in the rectangle $[0, T_1[\times[0, T_2[$. Since $\hat{v}$ owns a simple behaviour in this rectangle, we need relatively few grid points to represent this function sufficiently accurate. Nevertheless, the original signal $v(t)$ can be completely reconstructed by $\hat{v}$ via

$$v(t) = \hat{v}(t, t). \tag{3}$$

Thus we obtain an efficient multidimensional model of the time-dependent signal. The new representation (2) is called the *multivariate function* (*MVF*) of the multitone signal (1).

More general, we assume frequency modulation in addition to amplitude modulation. The signal

$$w(t) = \left[1 + \tfrac{1}{2}\sin\left(\tfrac{2\pi}{T_1}t\right)\right]\sin\left(\tfrac{2\pi}{T_2}t + \beta\sin\left(\tfrac{2\pi}{T_1}t\right)\right) \tag{4}$$

for $T_1 \gg T_2$, $\beta > 0$ includes both phenomena introduced by the slower time scale. Fig. 1 illustrates the qualitative behaviour of this signal. A multidimensional representation is directly given by the biperiodic function

$$\hat{w}_1(t_1, t_2) = \left[1 + \tfrac{1}{2}\sin\left(\tfrac{2\pi}{T_1}t_1\right)\right]\sin\left(\tfrac{2\pi}{T_2}t_2 + \beta\sin\left(\tfrac{2\pi}{T_1}t_1\right)\right). \tag{5}$$

Fig. 1 also shows this MVF. Unfortunately, many oscillations occur in the underlying rectangle. The number of oscillations even increases with the amount of frequency modulation, i.e. the larger the parameter β becomes. Thus the representation (5) is inefficient.

Narayan and Roychowdhury [7] propose an alternative strategy by modelling the frequency modulation separately. Consequently, we consider the MVF

$$\hat{w}_2(t_1, t_2) = \left[1 + \tfrac{1}{2}\sin\left(\tfrac{2\pi}{T_1}t_1\right)\right]\sin\left(2\pi t_2\right), \tag{6}$$

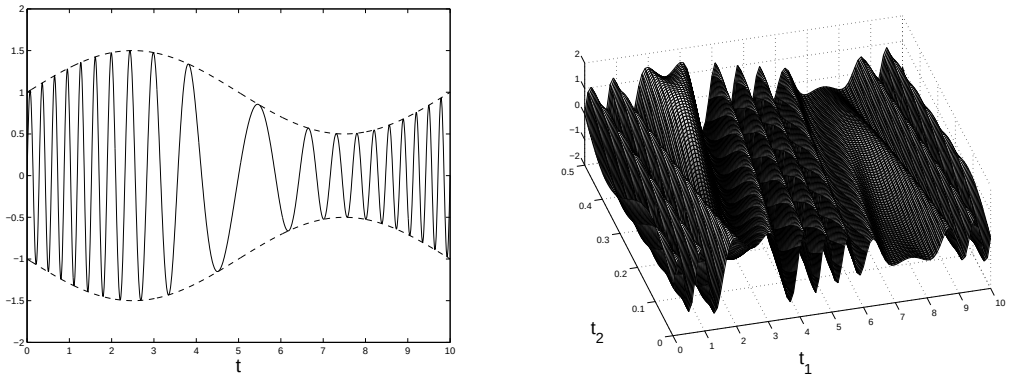

Figure 1: Frequency modulated signal w and unsophisticated MVF $\hat{w}_1$.

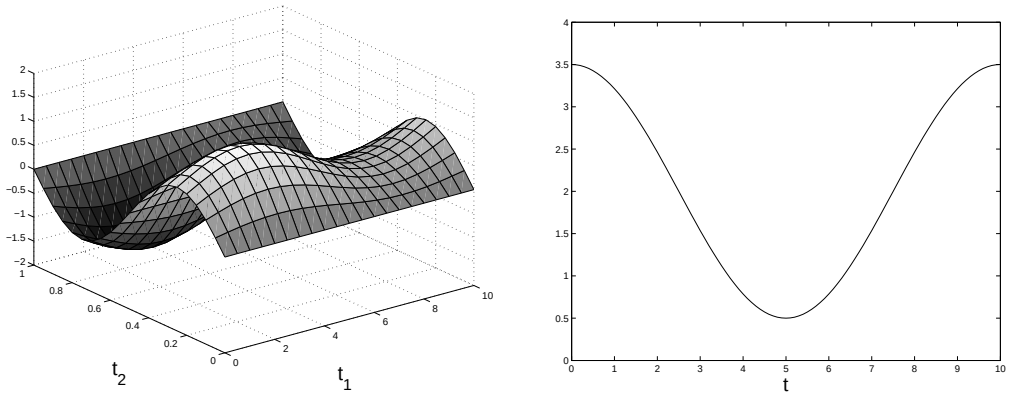

Figure 2: MVF $\hat{w}_2$ and corresponding local frequency ν.

where the second period is transformed to 1. This MVF is of the type (2). The frequency modulation is described by the function

$$\Psi(t) = \frac{t}{T_2} + \frac{\beta}{2\pi} \sin\left(\tfrac{2\pi}{T_1} t\right). \tag{7}$$

Its derivative Ψ' can be interpreted as the *local frequency* ν of the signal (4). In our case, we obtain

$$\nu(t) = \Psi'(t) = \frac{1}{T_2} + \frac{\beta}{T_1} \cos\left(\tfrac{2\pi}{T_1} t\right). \tag{8}$$

Hence the local frequency is T_1-periodic. Fig. 2 shows both MVF and local frequency. We recognise that these functions own an elementary behaviour now. The reconstruction of the original signal reads

$$w(t) = \hat{w}_2(t, \Psi(t)), \tag{9}$$

where the function Ψ stretches the second time scale. Therefore we call Ψ a *warping function*. In the representation (5), the corresponding warping function is linear, whereas the MVF is complicated. On the other hand, the nonlinear warping function (7) produces an efficient description by the MVF.

More general, the multidimensional model can be introduced for a frequency modulated quasiperiodic signal $\mathbf{x}(t) \in \mathbb{R}^n$ of the form

$$\mathbf{x}(t) = \sum_{j_1, j_2 = -\infty}^{\infty} \mathbf{X}_{j_1, j_2} \exp\left(i \left(\tfrac{2\pi}{T_1} j_1 t + 2\pi j_2 \Psi(t)\right)\right) \tag{10}$$

with constant coefficients $\mathbf{X}_{j_1,j_2} \in \mathbb{C}^n$ and warping function $\Psi(t) \in \mathbb{R}$.

3 Warped MPDAE

In circuit simulation, the transient behaviour of all node voltages and some branch currents is calculated. Modified nodal analysis [2] typically gives a system of *differential algebraic equations* (*DAEs*), which we write as

$$\tfrac{d}{dt}\mathbf{q}(\mathbf{x}) = \mathbf{f}(\mathbf{b}(t), \mathbf{x}(t)). \tag{11}$$

Thereby, $\mathbf{x} : \mathbb{R} \to \mathbb{R}^k$ denotes unknown voltages and currents. The function $\mathbf{q} : \mathbb{R}^k \to \mathbb{R}^k$ represents charges and fluxes. The right-hand side $\mathbf{f} : \mathbb{R}^l \times \mathbb{R}^k \to \mathbb{R}^k$ also depends on input signals $\mathbf{b} : \mathbb{R} \to \mathbb{R}^l$.

If the input signals are replaced by constant mean values $\mathbf{b}_0 \approx < \mathbf{b}(t) >$, then an autonomous DAE

$$\frac{d}{dt}\mathbf{q}(\mathbf{x}) = \mathbf{f}(\mathbf{b}_0, \mathbf{x}(t)) \tag{12}$$

arises. We assume that this DAE has a periodic solution $\mathbf{x}_{per}$. The corresponding period T_0 is unknown a priori. Since the DAE is autonomous, the relocated periodic function

$$\mathbf{y}(t) := \mathbf{x}_{per}(t + c) \tag{13}$$

also satisfies (12) for any fixed $c \in \mathbb{R}$. We can apply time or frequency domain methods to determine such a solution and its period [6]. In time domain, a phase condition like

$$\frac{d}{dt}\mathbf{x}^1(0) = 0 \tag{14}$$

without loss of generality for the first component of the solution has to be added to extract a special solution from the continuum (13). A nonconstant periodic function $\mathbf{x}^1 \in C^1$ possesses several points of the form (14) and they are isolated in general.

Now let the input signals $\mathbf{b}$ be periodic with time rate T_1. Therefore they produce a driven oscillation. In addition, the system (11) shall include a second inherent time scale. The input signals may vary this time scale, i.e. frequency modulation occurs. Consequently, a quasiperiodic solution of the form (10) arises. In numerical simulation, we want to use the multidimensional signal model. The transition to functions in several variables changes the DAE system of the circuit into a partial DAE system. Accordingly, the *warped multirate partial differential algebraic equation* (*MPDAE*) [7, 11] corresponding to (11) is defined as

$$\frac{\partial \mathbf{q}(\hat{\mathbf{x}})}{\partial t_1} + \nu(t_1)\frac{\partial \mathbf{q}(\hat{\mathbf{x}})}{\partial t_2} = \mathbf{f}(\mathbf{b}(t_1), \hat{\mathbf{x}}(t_1, t_2)) \tag{15}$$

with the MVF $\hat{\mathbf{x}}$ of $\mathbf{x}$. The input signals $\mathbf{b}$ are just T_1-periodic and thus do not require a multidimensional description. Since the input signals cause the frequency modulation, the local frequency function ν depends on the first variable and is also T_1-periodic. Generalisations to MPDAEs including several forced and several inherent time scales can directly be performed. For simplicity, we restrict to the frequent case (15).

It is straightforward to show that a solution $\hat{\mathbf{x}}$ of (15) yields a solution $\mathbf{x}$ of (11) via

$$\mathbf{x}(t) = \hat{\mathbf{x}}(t, \Psi(t)) \quad \text{with} \quad \Psi(t) = \int_0^t \nu(\tau)\, d\tau. \tag{16}$$

In addition, a biperiodic solution $\hat{\mathbf{x}}$ results in a frequency modulated quasiperiodic signal $\mathbf{x}$ of the form (10). It is difficult to verify the existence of a quasiperiodic solution for a given DAE (11). Nevertheless, the physical background often indicates such solution types. If no quasiperiodic solution exists, then at least

similar functions, especially in case of widely separated time scales. Thus the quasiperiodic response appears as an idealisation. The existence and uniqueness of quasiperiodic DAE solutions is closely connected to the existence and uniqueness of multiperiodic MPDAE solutions, see [10].

The warped MPDAE (15) is autonomous in the second time scale. It follows that a specific solution $\hat{\mathbf{x}}$ produces a continuum of solutions

$$\hat{\mathbf{y}}(t_1, t_2) := \hat{\mathbf{x}}(t_1, t_2 + c) \tag{17}$$

for each $c \in \mathbb{R}$. Since this translation preserves the periodicities, we have to isolate special biperiodic solutions.

The crucial problem of the warped MPDAE (15) is that the local frequency ν represents an a priori unknown function. The resulting warping function Ψ shall produce an efficient multidimensional description of the quasiperiodic solution. Since there exists no a priori knowledge about the solution in general, we are not able to choose a local frequency function. Thus we hold the local frequency as an unknown function and deal with the underdetermined system (15). In the previous section, we have seen that the warping function is not unique.

In RF applications, the forced time rate is often much slower than the autonomous time scale, i.e. $T_1 \gg \nu(t_1)^{-1}$ holds for all t_1. Due to the periodicity, we have to determine the values $\nu(t_1)$ for $t_1 \in [0, T_1[$. Accordingly, a continuous condition has to be posed, which determines the local frequency. One can try to demand a condition, where the local frequency is directly involved. Another idea is to determine the local frequency indirectly using the corresponding solution $\hat{\mathbf{x}}$, which leads to a continuous phase condition in the multidimensional time domain. We consider a single component of the solution, without loss of generality the first component $\hat{\mathbf{x}}^1(t_1, t_2)$. In [7], the authors propose to prescribe the derivative

$$\frac{\partial \hat{\mathbf{x}}^1}{\partial t_2}(t_1, 0) = \eta(t_1) \quad \text{for all } t_1 \in \mathbb{R} \tag{18}$$

as a slowly varying T_1-periodic function η. Conditions of this form shall prevent the solution from being highly oscillatory. The choice of the line $t_2 = 0$ is arbitrary due to the degree of freedom by translation in this coordinate direction. The phase condition (18) can be added to the biperiodic boundary conditions in the domain of dependence. However, we often do not have a priori knowledge how to choose the function η to ensure the existence of a solution.

Another possibility is to arrange a minimum condition [4]. In general, a solution of (15) exists, which satisfies an appropriate minimum condition. Yet the computational effort for numerical simulation increases significantly in comparison to requirements like (18).

To avoid these difficulties, we propose a special choice for the phase condition. Test results show that in the majority of cases solutions exist, which satisfy

$$\frac{\partial \hat{\mathbf{x}}^1}{\partial t_2}(t_1, t_2^0) = 0 \tag{19}$$

for all $t_1 \in \mathbb{R}$ and some $t_2^0 \in \mathbb{R}$. We find these phenomena in the case of two forced time scales, too. In our example from the previous section, the unsophisticated MVF (5) does not fulfil (19) for any t_2, while the appropriate MVF (6) satisfies the condition for $t_2^0 = \frac{\pi}{2}, \frac{3\pi}{2}$. Using the degree of freedom by translation in the second coordinate direction, we strengthen the phase condition (18) to

$$\frac{\partial \hat{\mathbf{x}}^1}{\partial t_2}(t_1, 0) = 0 \quad \text{for all } t_1 \in \mathbb{R}. \tag{20}$$

This phase condition is heuristic and thus the existence of corresponding solutions can not be guaranteed. However, the physical behaviour of signals indicates that the choice is reasonable. The continuous phase condition (20) can be seen as a multidimensional generalisation of the phase condition (14) for autonomous DAEs.

A special case arises, if the local frequency is constant, i.e. $\nu(t_1) \equiv \nu_0 \in \mathbb{R}$. Accordingly, the warped MPDAE (15) becomes

$$\frac{\partial \mathbf{q}(\hat{\mathbf{x}})}{\partial t_1} + \nu_0 \frac{\partial \mathbf{q}(\hat{\mathbf{x}})}{\partial t_2} = \mathbf{f}(\mathbf{b}(t_1), \hat{\mathbf{x}}(t_1, t_2)), \tag{21}$$

which corresponds to a standard MPDAE, cf. [1]. The frequency ν_0 represents a scalar unknown here. Now we just have to add a phase condition like

$$\frac{\partial \hat{\mathbf{x}}^1}{\partial t_2}(0, 0) = 0 \tag{22}$$

to isolate a solution from the family (17) and to determine the unknown frequency. Thereby, the advantage is that solutions satisfying (22) do exist such as in the DAE case using (14). Thus if a biperiodic solution of (21) exists, then some translated functions via (17) also fulfil (22).

We can simulate the case of constant local frequency in the MPDAE model (15) as well as (21). In general, a solution of (15) does not exhibit a constant local frequency, since the input signals also influence the second time scale. Nevertheless, we may use the model (21) as an idealisation, if $\nu(t_1) \approx \nu_0$ holds approximately. However, we can not apply standard perturbation theory here, since the properties of the solution change not only quantitatively but qualitatively.

4 Method of Characteristics

Now we analyse the information transport in the warped MPDAE system (15). Each equation owns the form

$$(1, \nu(t_1)) \cdot \left(\frac{\partial \mathbf{q}^i(\hat{\mathbf{x}})}{\partial t_1}, \frac{\partial \mathbf{q}^i(\hat{\mathbf{x}})}{\partial t_2} \right)^T = \mathbf{f}^i(\mathbf{b}(t_1), \hat{\mathbf{x}}(t_1, t_2)) \tag{23}$$

for the components $i = 1, \ldots, k$. Hence the left-hand side represents the derivative of $\mathbf{q}^i(\hat{\mathbf{x}})$ in direction $(1, \nu(t_1))$. Accordingly, we define a *characteristic system* of the warped MPDAE (15) as the following equations

$$\begin{aligned} \tfrac{d}{d\tau} t_1(\tau) &= 1 \\ \tfrac{d}{d\tau} t_2(\tau) &= \nu(t_1(\tau)) \\ \tfrac{d}{d\tau} \mathbf{q}(\bar{\mathbf{x}}(\tau)) &= \mathbf{f}(\mathbf{b}(t_1(\tau)), \bar{\mathbf{x}}(\tau)), \end{aligned} \tag{24}$$

where the variables t_1, t_2 and the solution $\bar{\mathbf{x}}$ depend on a parameter τ. The system (24) implies a family of DAEs and particular solutions are called *characteristic curves*. Given a local frequency function ν, we solve the part for the variables t_1, t_2 explicitly and obtain the *characteristic projections*

$$\begin{aligned} t_1 &= \tau + c_1 \\ t_2 &= \Psi(t_1) + c_2 \quad \text{with} \quad \Psi(t_1) = \int_0^{t_1} \nu(\tau)\, d\tau \end{aligned} \tag{25}$$

for arbitrary $c_1, c_2 \in \mathbb{R}$. These projections form a continuum of parallel curves in the domain of dependence. If the function ν is periodic, continuous and positive, then the resulting warping function Ψ becomes bijective.

It follows that solutions of the warped MPDAE are composed of characteristic curves. Furthermore, Cauchy initial value problems are solvable under the usual conditions. The proofs operate like for the ODE case analysed in [8]. Hence the characteristic system (24) completely describes the information transport in the warped MPDAE system (15).

Our aim is to determine a $(T_1, 1)$-periodic solution $\hat{\mathbf{x}}$ of (15) together with its T_1-periodic local frequency ν, where $T_1 \gg \nu^{-1}$ holds. Since the second period is transformed to 1, the frequency function includes the magnitudes of the second time scale. To construct an according method of characteristics, we perform the following discretisation. In the rectangle $[0, T_1] \times [0, 1]$, we choose the initial points

$$(t_{1,j}, t_{2,j}) = ((j-1)h, 0) \quad \text{for} \quad j = 1, \ldots, n \quad \text{and} \quad h = T_1/n. \tag{26}$$

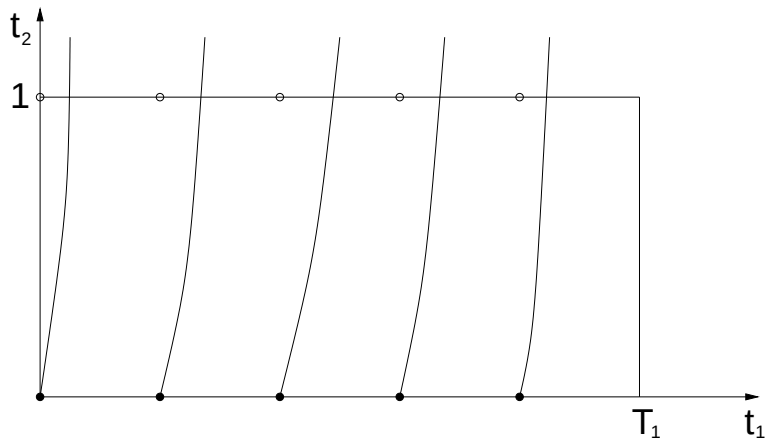

Figure 3: Characteristic projections in domain of dependence.

For a fixed local frequency function, a unique characteristic projection passes through each point, see Fig. 3. Consequently, we extract the corresponding equations from the characteristic system (24), which are

$$\tfrac{d}{d\tau}\mathbf{q}(\tilde{\mathbf{x}}_j(\tau)) = \mathbf{f}(\mathbf{b}(\tau + (j-1)h), \tilde{\mathbf{x}}_j(\tau)) \quad \text{for} \quad j = 1, \ldots, n. \tag{27}$$

These equations represent a collection of n DAE subsystems for the restrictions $\tilde{\mathbf{x}}_j$. Initial values in the points (26) correspond to the parameter $\tau = 0$ for each j. They determine the solution along the characteristic projections via the systems (27).

The characteristic projections themselves are given by the local frequency function. According to (26), we also discretise the local frequency to obtain a finite set of values $\nu(t_{1,j})$ for $j = 1, \ldots, n$.

Integrating the characteristic systems (27) yields final values on the line $t_2 = 1$, which correspond to different parameters $\tau = \tau_j$ for each subsystem. We use these final values to interpolate the solution in the opposite points $((j-1)h, 1)$. Hence the periodicity in the second coordinate direction generates boundary conditions

$$\left(\tilde{\mathbf{x}}_1(0)^T, \ldots, \tilde{\mathbf{x}}_n(0)^T\right)^T = \mathcal{B}\left(\tilde{\mathbf{x}}_1(\tau_1)^T, \ldots, \tilde{\mathbf{x}}_n(\tau_n)^T\right)^T, \tag{28}$$

where $\mathcal{B} \in \mathbb{R}^{nk \times nk}$ is a matrix. Thereby, the periodicity in the first coordinate direction is also applied to identify points at the boundaries. Both $\mathcal{B}$ and the end points $\tau_1, \ldots, \tau_n$ depend on the local frequency and thus are unknown a priori. However, for given starting values $\nu(t_{1,j})$, we can approximate the characteristic projections. For example, using trapezoidal rule in the integration (25) is equivalent to approximating the characteristic projections by piecewise quadratic polynomials. Consequently, the equations (28) can be evaluated, which enables a numerical scheme.

Hence the method of characteristics results in a boundary value problem of DAEs (27),(28). The DAE subsystems are independent from each other, since they correspond to different characteristic curves. Just the boundary conditions cause a coupling between the subsystems. Therefore the described technique leads to drastic reductions of computational work in comparison to standard PDAE techniques [9]. If the MPDAE (15) corresponds to an underlying ODE, then the subsystems (27) also represent ODEs and the interpolation (28) is uncritical. In the DAE case, modifications may be necessary to differ between free and dependant components of the solution.

The problem (27),(28) is still underdetermined, since the values $\nu(t_{1,j})$ are unknown. Thus we have to include the phase condition (20) in the discretised form

$$\frac{\partial \hat{\mathbf{x}}^1}{\partial t_2}(t_{1,j}, 0) = 0 \quad \text{for} \quad j = 1, \ldots, n. \tag{29}$$

The information transport via the characteristic curves performs in the direction $(1, \nu)$, whereas the condition (29) represents a derivative in direction $(0, 1)$. Hence we can not directly add the phase condition (29) to the boundary conditions (28) for the restrictions $\tilde{\mathbf{x}}_j$. Therefore we assume that the derivative of the first component is explicitly given in the underlying DAE system (11)

$$\frac{d\mathbf{x}^1}{dt} = \mathbf{f}^1(\mathbf{b}(t), \mathbf{x}). \tag{30}$$

The corresponding equation in the MPDAE system (15) yields an alternative now. If we replace the derivative in the first coordinate direction by a difference formula, e.g. centred differences, then it follows the approximation

$$\begin{aligned} \nu(t_{1,j}) \frac{\partial \hat{\mathbf{x}}^1}{\partial t_2}(t_{1,j}, 0) \;&\doteq\; \mathbf{f}^1(\mathbf{b}(t_{1,j}), \hat{\mathbf{x}}(t_{1,j}, 0)) \\ &\quad - \tfrac{1}{2h} \left[\hat{\mathbf{x}}^1(t_{1,j+1}, 0) - \hat{\mathbf{x}}^1(t_{1,j-1}, 0)\right] \end{aligned} \tag{31}$$

for $j = 1, \ldots, n$. We use the periodicity in the first coordinate direction to eliminate the unknowns for $j = 0, n+1$. Consequently, (29) and $\nu > 0$ imply the conditions

$$\mathbf{f}^1(\mathbf{b}(t_{1,j}), \hat{\mathbf{x}}(t_{1,j}, 0)) - \tfrac{1}{2h} \left[\hat{\mathbf{x}}^1(t_{1,j+1}, 0) - \hat{\mathbf{x}}^1(t_{1,j-1}, 0)\right] = 0 \tag{32}$$

for all $j = 1, \ldots, n$. Thereby, only initial values $\tilde{\mathbf{x}}_j(0)$ arise in the equations (32). Thus we add these equations to the boundary conditions (28). Consequently, the problem includes as many boundary conditions as unknown functions and frequency values.

To solve the complete task, one can apply techniques for boundary value problems of DAEs, e.g. shooting methods [12]. In corresponding Newton iterations for

solving nonlinear systems, we require appropriate starting values for the solution and the local frequency. Otherwise the iterations may not converge at all. If we replace the input signals $\mathbf{b}(t)$ by constant mean values $\mathbf{b}_0$, then we obtain the autonomous DAE (12). We compute a periodic solution $\mathbf{x}_{per}(t)$ with phase condition $\dot{\mathbf{x}}^1_{per}(0) = 0$ and its period T_0. This signal owns a trivial extension to a MVF via $\hat{\mathbf{x}}_{per}(t_1, t_2) = \mathbf{x}_{per}(t_2)$. We can apply this MVF and the local frequency $\nu(t_1) \equiv T_0^{-1}$ as starting values in the Newton iteration. Unfortunately, often this choice is still not sufficient for the convergence.

Therefore we construct a homotopy method, which shall provide for convergence of the Newton iterations. We consider the family of warped MPDAEs

$$\frac{\partial \mathbf{q}(\hat{\mathbf{x}})}{\partial t_1} + \nu(t_1)\frac{\partial \mathbf{q}(\hat{\mathbf{x}})}{\partial t_2} = \mathbf{f}(\lambda(\mathbf{b}(t_1) - \mathbf{b}_0) + \mathbf{b}_0, \hat{\mathbf{x}}) \tag{33}$$

including the homotopy parameter $\lambda \in [0, 1]$. The solution $\hat{\mathbf{x}}$ and the local frequency ν depend on this parameter. The MVF $\hat{\mathbf{x}}_{per}$ together with $\nu(t_1) \equiv T_0^{-1}$ satisfies the MPDAE for $\lambda = 0$ and the continuous phase condition (20). For $\lambda = 1$, we obtain the desired solution. Accordingly, small step sizes in the parameter λ ensure that the solution in one step represents good starting values for the subsequent step. The homotopy method is based on the MPDAE model. Hence we can use this strategy in any numerical scheme for solving biperiodic boundary value problems of (15). The physical interpretation of this technique is to supply the electrical circuit with appropriate input signals.

5 Van der Pol Oscillator

To apply the discussed model and the constructed method, we consider a forced Van der Pol oscillator as benchmark

$$\frac{d^2x}{dt^2} + \mu(x^2 - 1)\frac{dx}{dt} + \kappa^2 x = A \sin\left(\tfrac{2\pi}{T_1} t\right). \tag{34}$$

The autonomous oscillator ($A = 0$) exhibits a periodic solution. Now the input signal on the right-hand side introduces another time scale. Consequently, we change to the multidimensional model.

The simulation uses the equivalent ODE system of first order. We set up the resulting warped MPDE system and demand the continuous phase condition (20) for the first component. Using the method of characteristics from the previous section, we compute a biperiodic solution and corresponding local frequency. Linear interpolation is applied at the boundaries. A boundary value problem of ODEs arises, which we solve by a shooting method. Thereby, the trapezoidal rule performs the integration. Hence the complete method is consistent of order two.

Firstly, we observe a stiff case with the parameters

$$\mu = 10,\ \kappa = 2\pi,\ A = 30,\ T_1 = 1000.$$

Fig. 4 illustrates the resulting biperiodic solution and its local frequency. We obtain the corresponding solution of (34) via (9) by interpolation using the computed MVF values. Fig. 5 shows this solution in two time intervals. For comparison, the pictures also include the solution of an initial value problem, which is computed by the trapezoidal rule, too. In the first few cycles, the functions demonstrate a good agreement. In later cycles, a phase shift occurs between the signals. This phase shift is generated by small numerical errors in the local frequency, which amplify during many oscillations. Nevertheless, the other signal properties also agree in this region.

Secondly, we consider a nonstiff case with parameters

$$\mu = 0.1,\ \kappa = 2\pi,\ A = 30,\ T_1 = 1000.$$

The computed MVF and its local frequency is shown in Fig. 6. We observe a larger amount of amplitude modulation and less steep gradients as in the stiff case. Interestingly, the frequency modulation vanishes here, i.e. the local frequency represents a constant function. In this case, we can apply the idealised model (21), where the local frequency is set to a constant value ν_0. We also compute the corresponding PDE solution, where the scalar phase condition (22) is used. Thereby, the MVF exhibits the same form as in Fig. 6 and the frequency results in $\nu_0 = 0.9996$.

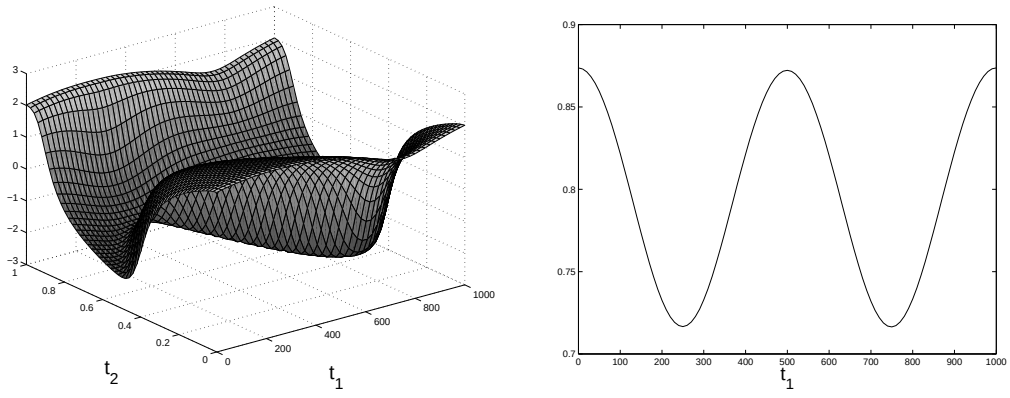

Figure 4: MVF (left) and local frequency (right) of solution for Van der Pol oscillator in the stiff case.

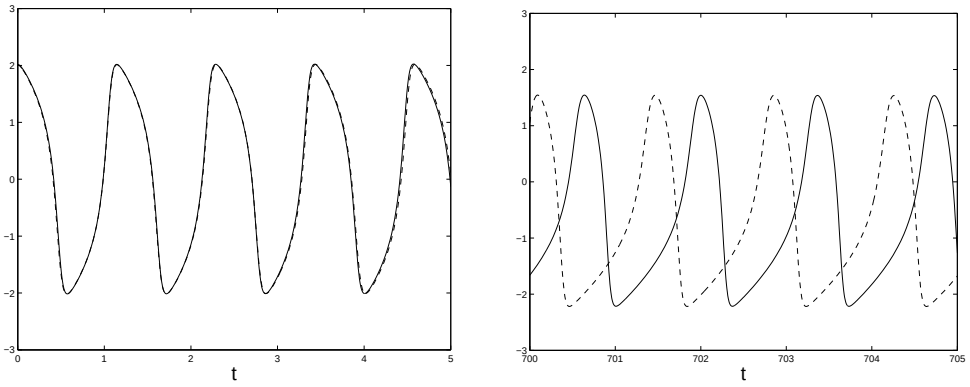

Figure 5: ODE solution for Van der Pol oscillator in the stiff case integrated by trapezoidal rule (solid line) and interpolated from MPDE solution (dashed line) in the intervals $[0, 5]$ (left) and $[700, 705]$ (right).

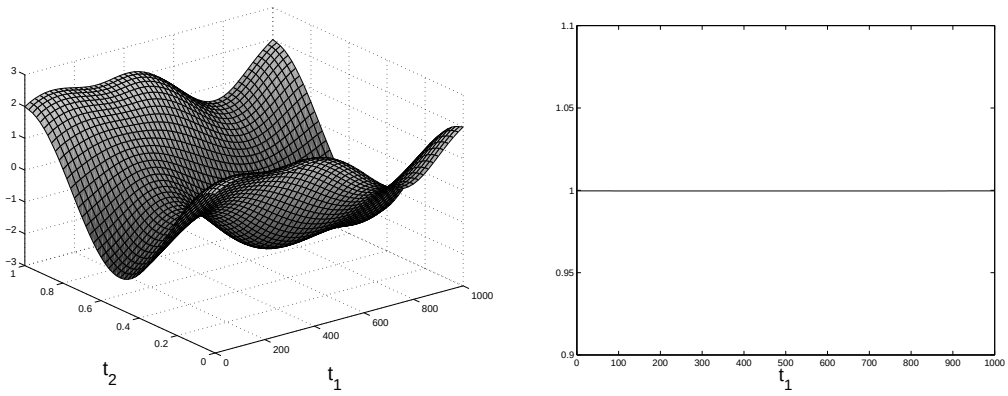

Figure 6: MVF (left) and local frequency (right) of solution for Van der Pol oscillator in the nonstiff case.

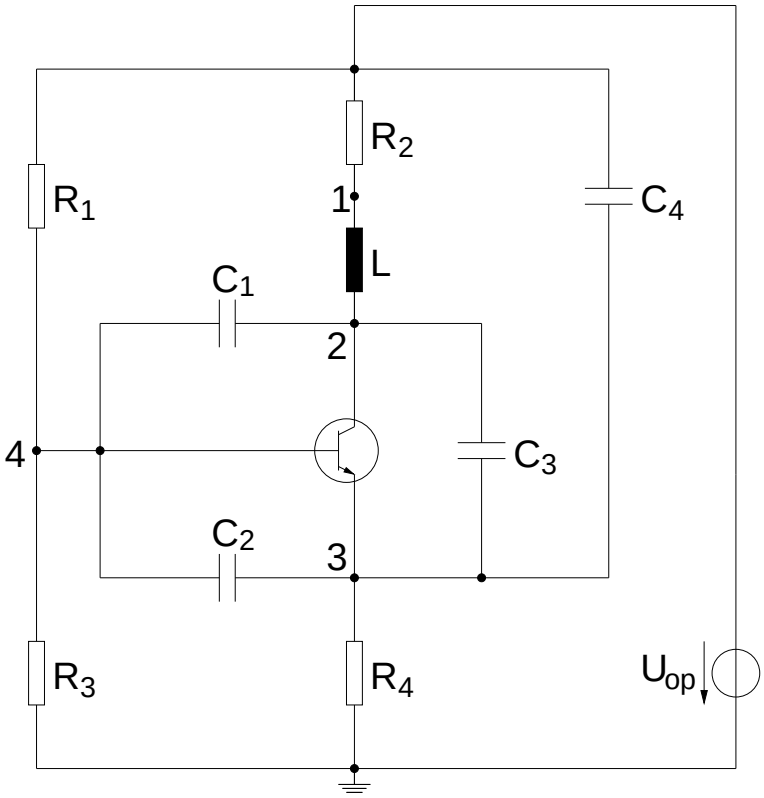

Figure 7: Circuit of Colpitt oscillator.

6 Colpitt Oscillator

To simulate a more complex electrical circuit, we examine a forced Colpitt oscillator. The Colpitt oscillator represents a typical LC-oscillator, see Fig. 7. The circuit includes one inductance, four capacitances and a bipolar transistor. The mathematical model of the Colpitt oscillator leads to an implicit ODE system, which describes the transient behaviour of four node voltages, namely

$$\begin{pmatrix} 1 & 0 & 0 & 0 \\ 0 & C_1+C_3 & -C_3 & -C_1 \\ 0 & -C_3 & C_2+C_3+C_4 & -C_2 \\ 0 & -C_1 & -C_2 & C_1+C_2 \end{pmatrix} \begin{pmatrix} \dot{U}_1 \\ \dot{U}_2 \\ \dot{U}_3 \\ \dot{U}_4 \end{pmatrix} = \tag{35}$$

$$\begin{pmatrix} \frac{R_2}{L}(U_2-U_1)+R_2\dot{U}_{op} \\ \frac{1}{R_2}(U_{op}-U_1)+\left(I_S+\frac{I_S}{b_C}\right)g(U_4-U_2)-I_S g(U_4-U_3) \\ -\frac{1}{R_4}U_3+\left(I_S+\frac{I_S}{b_E}\right)g(U_4-U_3)-I_S g(U_4-U_2) \\ -\frac{1}{R_3}U_4+\frac{1}{R_1}(U_{op}-U_4)-\frac{I_S}{b_E}g(U_4-U_3)-\frac{I_S}{b_C}g(U_4-U_2) \end{pmatrix}.$$

The applied transistor model includes the nonlinear function

$$g(U) = \exp\left(\frac{U}{U_T}\right) - 1. \tag{36}$$

The technical parameters are set to the values

$$\begin{aligned} &C_1 = 50 \text{ pF},\ C_2 = 1 \text{ nF},\ C_3 = 50 \text{ nF},\ C_4 = 100 \text{ nF},\ R_1 = 12 \text{ k}\Omega, \\ &R_2 = 3\ \Omega,\ R_3 = 8.2 \text{ k}\Omega,\ R_4 = 1.5 \text{ k}\Omega,\ L = 10 \text{ mH},\ U_{op} = 10 \text{ V}, \\ &I_S = 1 \text{ mA},\ b_E = 100,\ b_C = 50,\ U_T = 25.85 \text{ mV}. \end{aligned}$$

Using these parameters, the Colpitt oscillator owns a periodic solution with time rate $T_0 = 0.125$ ms. More details about the modelling of the Colpitt oscillator can be found in [5].

Now an external source controls the third capacitor

$$C_3(t) = 50 \text{ nF}\left(1 + 0.8 \sin\left(\tfrac{2\pi}{T_1} t\right)\right) \tag{37}$$

and we choose $T_1 = 1$ s. Hence the capacitance matrix in (35) becomes time-dependent and the system is no longer of the form (11). However, a regular capacitance matrix always arises. Thus the system (35) is equivalent to an explicit ODE, which represents a special case of (11).

In the multidimensional model, we use the method of characteristics the same way as described in the previous section. Fig. 8 shows the computed local frequency. According to an LC-oscillator, the frequency increases for lower capacitances. Fig. 9 illustrates the MVFs for the voltages U_1 and U_4. The corresponding ODE solutions are given in Fig. 10 and Fig. 11, respectively. A reference solution is computed by integrating the system (35) via the RADAU5 method [3]. We see no difference between both signals in the first few cycles. Later the numerical errors in the local frequency produce the said phase shift. Other signal properties are resolved correctly.

This example illustrates the advantage of the multidimensional model with respect to the computational effort. In the corresponding signals, more than 8000 oscillations arise during the time interval $[0, T_1]$. An integration scheme using the ODE model has to resolve all these oscillations. On the other hand, we compute the PDE solution along 100 characteristic curves, where just a single oscillation is integrated on each curve. Furthermore, we obtain a compact visualisation of the signals by their MVFs and the local frequency, whereas the ODE solutions need to be zoomed in relatively small time intervals for a detailed discussion.

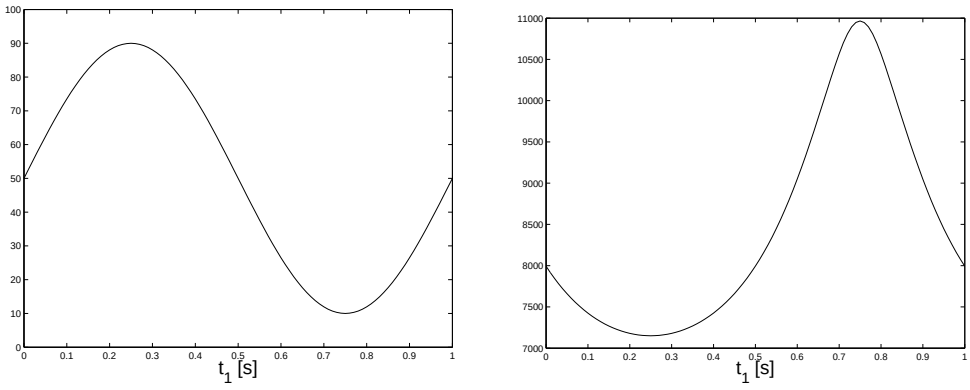

Figure 8: Input signal C_3[nF] (left) and local frequency $\nu[\mathrm{s}^{-1}]$ (right) of solution for Colpitt oscillator.

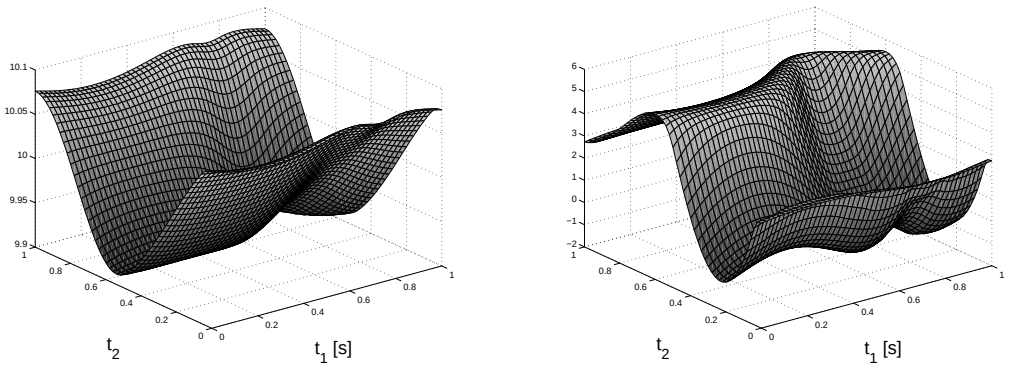

Figure 9: MVFs $\hat{U}_1$[V] (left) and $\hat{U}_4$[V] (right) in Colpitt oscillator.

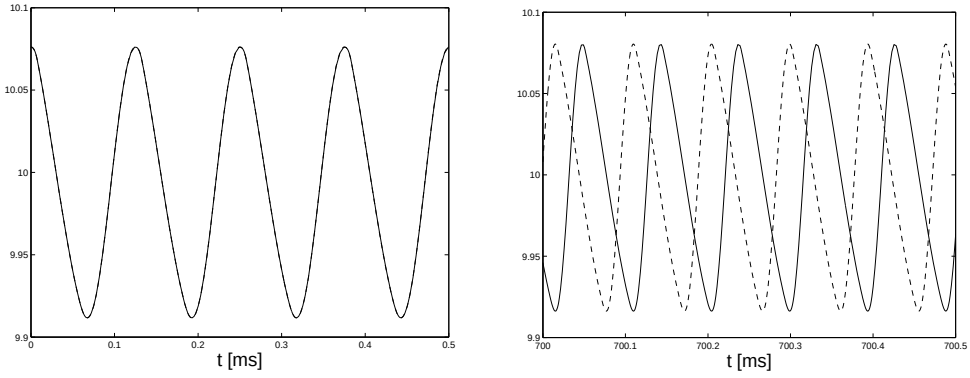

Figure 10: ODE solution U_1[V] of Colpitt oscillator integrated using RADAU5 (solid line) and interpolated from MPDE solution (dashed line) in time intervals $[0\mathrm{ms}, 0.5\mathrm{ms}]$ (left) and $[700\mathrm{ms}, 700.5\mathrm{ms}]$ (right).

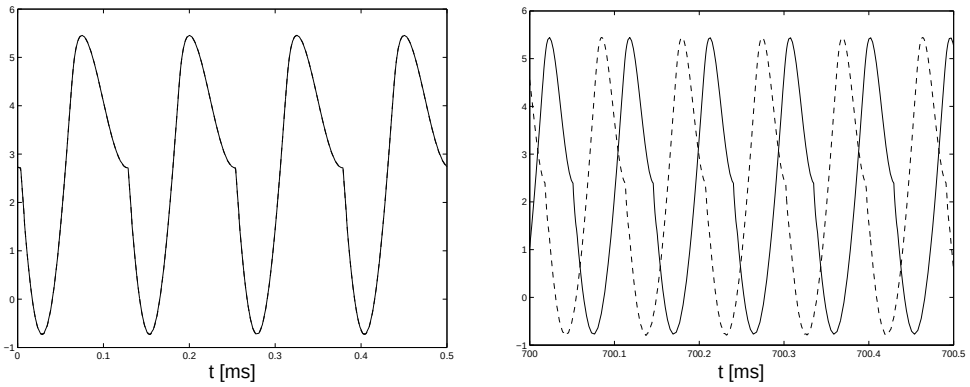

Figure 11: ODE solution U_4[V] of Colpitt oscillator integrated (solid line) and interpolated from MPDE solution (dashed line) in time intervals $[0\text{ms}, 0.5\text{ms}]$ (left) and $[700\text{ms}, 700.5\text{ms}]$ (right).

7 Conclusions

The warped MPDAE model provides an alternative strategy for the simulation of frequency modulated quasiperiodic signals. A heuristic choice of the required phase condition has been introduced. The information transport in the MPDAE system performs along characteristic curves, which yields a corresponding numerical technique for the arising boundary value problems. Test results confirm that the constructed method is suitable for simulating RF circuits, which include a mixture of widely separated driven and autonomous time rates. It is still open to examine, if appropriate assumptions can guarantee the existence of solutions, which satisfy the presented phase condition. Alternatively, this question may be easier to decide for other additional equations, e.g. minimum conditions.

Acknowledgements

This research has been supported by the Technical University of Munich. The author is indebted to Prof. Dr. P. Rentrop (Technical University of Munich), Prof. Dr. M. Günther (University of Wuppertal) and Dr. U. Feldmann (Infineon Technologies, Munich) for helpful discussions.

References

[1] Brachtendorf, H. G.; Welsch, G.; Laur, R.; Bunse-Gerstner, A.: Numerical steady state analysis of electronic circuits driven by multi-tone signals. Electrical Engineering 79 (1996), pp. 103-112.

[2] Günther, M.; Feldmann, U.: CAD based electric circuit modeling in industry I: mathematical structure and index of network equations. Surv. Math. Ind. 8 (1999), pp. 97-129.

[3] Hairer, E.; Wanner, G.: Solving Ordinary Differential Equations II. Stiff and Differential-Algebraic Problems. 2nd Ed., Springer, Berlin 1996.

[4] Houben, S.H.M.J.: Simulating multi-tone free-running oscillators with optimal sweep following. to appear in: Proceedings Conference Scientific Computing in Electrical Engineering, Eindhoven, 2002.

[5] Kampowsky, W.; Rentrop, P.; Schmitt, W.: Classification and numerical simulation of electric circuits. Surv. Math. Ind. 2 (1992), pp. 23-65.

[6] Kundert, K. S.; Sangiovanni-Vincentelli, A.; Sugawara, T.: Techniques for finding the periodic steady-state response of circuits. In: Ozawa, T. (Ed.): Analog methods for computer-aided circuit analysis and diagnosis. New York 1988, pp. 169-203.

[7] Narayan, O.; Roychowdhury, R.: Multi-time simulation of voltage-controlled oscillators. Proceedings Design Automation Conference, 1999, pp. 629-634.

[8] Pulch, R.; Günther, M.: A method of characteristics for solving multirate partial differential equations in radio frequency application. Appl. Numer. Math. 42 (2002), pp. 397-409.

[9] Pulch, R.: Finite difference methods for multi time scale differential algebraic equations. Z. Angew. Math. Mech. 83 (2003) 9, pp. 571-583.

[10] Roychowdhury, J.: Analysing circuits with widely-separated time scales using numerical PDE methods. IEEE Trans. CAS I 48 (2001) 5, pp. 578-594.

[11] Roychowdhury, J.: Multi-time PDEs for dynamical system analysis. In: Rienen, U. van; Günther, M.; Hecht, D. (Eds.): Scientific Computing in Electrical Engineering. Lecture Notes in Computational Science and Engineering, Springer 2001, pp. 3-14.

[12] Stoer, J.; Bulirsch, R.: Introduction to Numerical Analysis. 3rd Ed., Springer, New York 2002.